

Experimental observation of breakdowns in the Fermilab RF Gun G4 *

J.-P. Carneiro¹, D. Edwards², I. Gonin², S. Schreiber¹

¹ Deutsches Elektronen-Synchrotron, Notkestrasse 85, D-22607 Hamburg, Germany

² Fermi National Accelerator Laboratory, MS 306, P.O. Box 500, Batavia, IL 60510, USA

1. Introduction

Fermilab has developed and delivered to DESY Hamburg two RF guns for the operation of the phase I of the TESLA Test Facility (TTF) accelerator. The first RF gun (designated *G3* in the following) has been operated on TTF from October 1998 to March 2002. *G3* presented a reliable behaviour with short RF pulses ($< 300 \mu\text{s}$). For longer RF pulses, *G3* suffered from breakdowns occurring in the coupling slot located between the waveguide and the full-cell of the gun [1]. These breakdowns were followed by photo-multiplier or vacuum interlocks and for RF pulses longer than $500 \mu\text{s}$ the breakdowns rate increased to an unacceptable value. Therefore, a second RF gun (*G4*) has been installed in June 2002 on TTF. *G4* was in operation at the A0 photo-injector at Fermilab since January 1999 where it has been successfully conditioned at 1 Hz repetition rate for RF pulses up to $550 \mu\text{s}$. *G4* has been operated at DESY with long RF pulses (up to $900 \mu\text{s}$), high forward power (up to 2.8 MW) and a repetition rate ranging from 0.1 to 2.0 Hz. Similar to *G3*, breakdowns were observed at DESY during the operation of *G4* as well. This paper describes the dependency of the breakdowns measured at DESY on *G4* with respect to the RF pulse length, forward power and repetition rate. A part of the work presented in this paper is also discussed in the reference [2].

2. Description of the RF gun

A layout of the Fermilab RF gun *G4* is presented in figure 1. The RF gun consists in a OFHC copper structure of 1.625 cells resonating in the mode $\text{TM}_{010,\pi}$ at 1.3 GHz. The length of the half cell has been increased to $\frac{5}{4} \cdot \frac{\lambda_{HF}}{4}$ (instead of $\frac{\lambda_{HF}}{4}$) because previous studies [3] have shown that this modification betters the beam transverse emittance. The length of the full cell is exactly $\frac{\lambda_{HF}}{2}$.

G4 is a high duty cycle (1%) RF gun built to handle long RF pulses (up to $900 \mu\text{s}$), with 4.5 MW of peak power at 10 Hz repetition rate, producing at this regime a mean power of 42 kW. This heat is evacuated by water cooling machined in the cavity walls and allowing a water flow of 4 l/s at a pressure of 6 bars. Table 1 gives a summary of the main electrical properties of the RF gun.

Mode	$\text{TM}_{010\pi}$
Resonant Frequency f	1.3 GHz
Transit Time Factor T	0.73127
External Quality Factor Q_{ext}	23700
Shunt Impedance ZT^2	27.92 $\text{M}\Omega/\text{m}$
Ratio peak field to accelerating field E_0/E_a	1.87
Peak power for $E_0=35 \text{ MV/m}$	2.2 MW

Table 1: Main electrical properties of the Fermilab RF gun (from [4]).

* TESLA Note 2003-13, published in November 2003.

- A : WATER COOLING SYSTEM
- B : PHOTO-CATHODE LOCATION
- C : LOW ENERGY PLATE
- INTERFACE AIR/WATER
- D : LOW ENERGY PLATE
- INTERFACE WATER/VACUUM
- E : HIGH ENRGY PLATE
- INTERFACE VACUUM/WATER
- F : HIGH ENERGY PLATE
- INTERFACE WATER/VACUUM
- G : WAVEGUIDE
- H : COUPLING SLOT

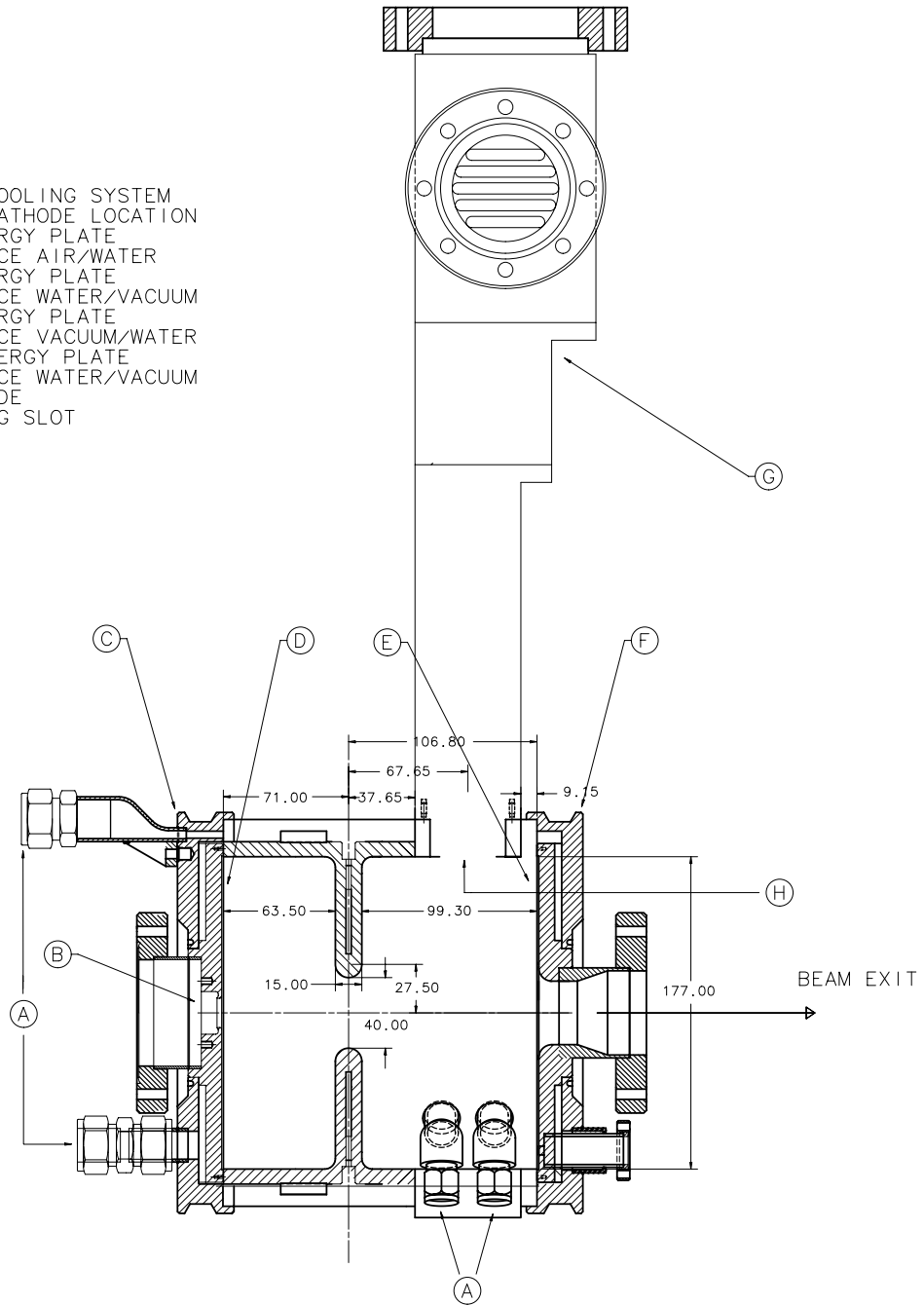


Fig. 1: The Fermilab RF Gun *G4*. Dimensions are in millimeters

Tuning of the RF gun

The tuning of *G4* has been done at Fermilab from May to July 1998. When first received from the Fermilab machine shop, *G4* was constituted of 6 different pieces: the main body of 1.625 cells, the waveguide and 4 plates (2 for the interface vacuum/water and 2 for the interface water/air). The tuning has been done in two steps:

The first step was to increase the diameter of the cells in order to decrease the resonant frequency of the cavity. At the reception of *G4* the diameter of the half and full cell were measured respectively at $\theta_i^{HC} = 176.959$ mm and $\theta_i^{FC} = 176.997$ mm and the frequency of the π mode at $f_i^\pi = 1309.176$ MHz. After two cuts, the diameter of the cells were increased to $\theta_f^{HC} = 178.206$ mm and $\theta_f^{FC} = 178.028$ mm thus decreasing the π mode frequency to $f_f^\pi = 1300.601$ MHz. The difference of frequency between the full and the half cell was measured at +722 kHz, necessary according to Superfish [5] simulations to keep a field of equal strength in both cells. Finally it is important to notify that the frequency of the π mode was kept 600 kHz too high in order to compensate the frequency variations expected while operating the gun under vacuum (-343 kHz), at 35°C (-220 kHz) and in the presence of water (+43 kHz due to the 6 bars of external pressure into the cavity walls). After the brazing of the 2 end plates vacuum/water into the main body, *G4* was ready for the second step of the tuning. The RF gun was strongly under-coupled ($\beta^{HF} = 0.56$) with a peak electric field on the full cell (E_{peak}^{FC}) slightly higher than the one on the half cell : ($E_{peak}^{FC}/E_{peak}^{HC}=1.02$).

The second step of the tuning consisted on a uniform aperture of the coupling slot in order to obtain a good coupling between the waveguide and the full-cell. A drawing of the coupling slot with its initial and final dimensions is shown in figure 2. Five cuts of the coupling slot have been necessary to bring the coupling from $\beta^{HF} = 0.56$ to $\beta^{HF} = 0.95$. Each cut has been done in the machine shop with a precision of 1 mil of an inch (0.0254 mm). The initial and final area of the coupling slot were respectively 378 mm² and 548 mm². During the cuts, no particular attention have been taken with respect to the edges of the slot. These edges were kept sharp. After the brazing of the waveguide and the two last end plates (water/air) on the main body of *G4*, the RF gun was slightly under-coupled (Standing Wave Ratio = 1.05) and a bead-pull measurement showed a field on the full cell higher than the one on the half cell: $E_{peak}^{FC}/E_{peak}^{HC} = 1.09$.

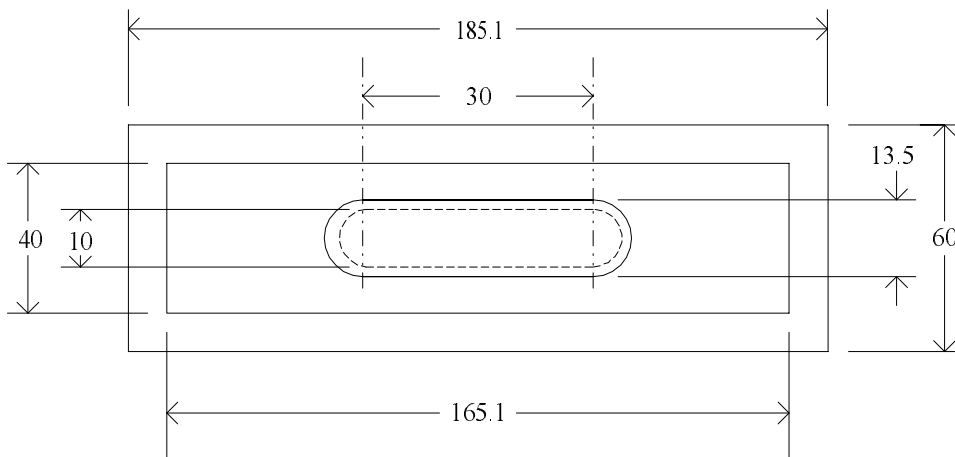


Fig. 2: Schematic view of the coupling slot. The dashed line represents the initial size of the slot before tuning. Dimensions are in millimeters. From Fermilab drawing ME-314580.

3. Operation of G4 at DESY

3.1 Installation

The exchange of RF guns on the TTF accelerator has been done in June 2002. *G4* was, as for *G3*, surrounded by three solenoids (a primary, a secondary and a bucking to zero the magnetic field on the cathode). The primary and the bucking solenoids were powered in series and a second power supply was used for the secondary solenoid. A layout of the RF system of the gun is presented in Figure 3. The main elements of this RF system are:

- An oscillator delivering a 9 dBm signal at a frequency of 1.3 GHz.
- A Vector Modulator controlled by a Unix station which determines the phase and the amplitude of the RF wave.
- A pre-amplifier and an amplifier with a gain of 20 and 30 dB respectively.
- A klystron delivering RF pulses up to 3.6 MW of peak power. During the experiments, we operated the klystron with a maximum repetition rate of 2 Hz and with pulse length up to 900 μ s.

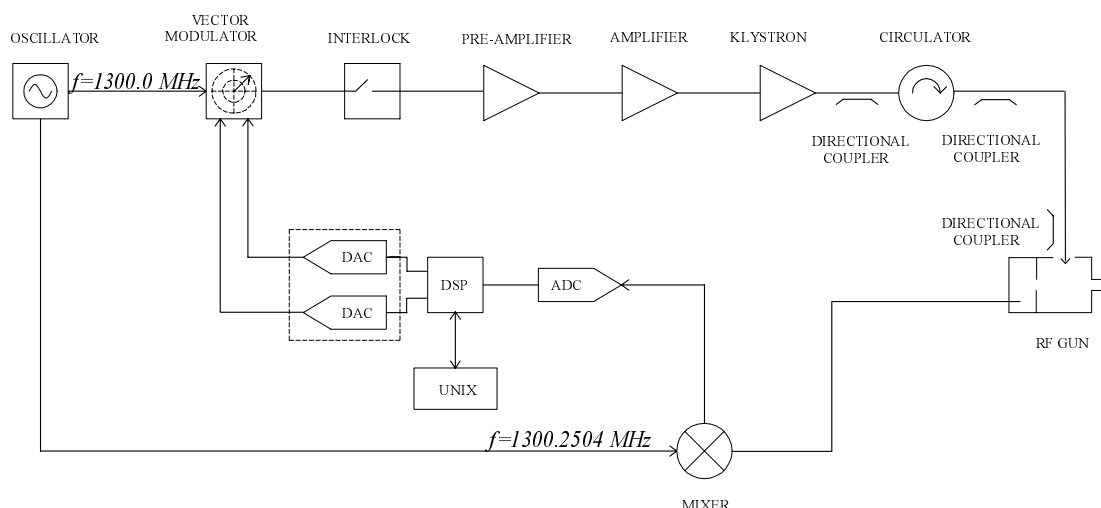


Fig. 3: RF system of the TTF RF Gun.

To protect the klystron from the gun reflected power, a circulator has been installed downstream of the klystron. Losses in the circulator has been measured at $\sim 20\%$. The maximum peak power going into the gun is therefore ~ 2.8 MW. A new air cooled RF window (not indicated in Figure 3) has been installed with *G4* together with a new waveguide (~ 1 meter long filled with SF_6) upstream the RF window.

A feedback loop maintains the phase and the amplitude of the RF wave constant into the gun. The transmitted power into the gun is measured by a probe located in the back plane of the half-cell of the gun and this signal is mixed with a reference signal of 1300.2504 MHz coming from the oscillator. The component of 250 kHz is sent to an Analog Digital Converter (ADC) and Digital Signal Processor (DSP) modules. This last module compares the phase and amplitude of the incoming signal with the desired one and make the compensations if necessary. The DSP output is sent to an Digital Analog Converter (DAC) module which treats the phase and amplitude signal as a complex vector.

As indicated in Figure 3, an interlock box is installed at the exit of the vector modulator. This interlock box prevents the operation of the RF system if any interlock (Photo-multiplier, vacuum, reflected power, SF_6 pressure, etc...) is fired.

3.2 Conditioning

The conditioning of *G4* at DESY has been done in July 2002 using a Mo cathode. Three days were necessary to condition *G4* at 500 μs , 3 MW, 1 Hz and for any combination of currents in the primary and secondary solenoids. The fact that the gun had been conditioned at Fermilab for these settings explain probably the ease of the conditioning. The conditioning up to 900 μs , 2.2 MW, 1 Hz and for any solenoids current took one additional week and was more difficult to achieve, mainly because of vacuum events detected by the ions pumps located at the waveguide of the RF gun and the 10 way cross. The threshold of these ion pumps was set to 3×10^{-9} mbar. For RF pulse lengths longer than 500 μs , we concentrated our efforts in the operation of *G4* at 2.2 MW which corresponds to a peak electric field on the RF gun of 35 MV/m, i.e high enough for the long pulses experiments foreseen at TTF.

Figure 4 shows the evolution of the dark current in *G4* during its operation at DESY, for a peak field of 35 MV/m and a current in the primary and secondary solenoids of respectively $I_p = 216$ A, and $I_s = 110$ A. The measurements has been done with a Cs_2Te photocathode, except for the first and last measurement done with a molybdenum and KCsTe photocathodes as indicated in Figure 4. The dark current has been measured using the Faraday cup located at the exit of the RF gun ($z \simeq 63$) cm from the photocathode. From Figure 4 we can see that the dark current presents some strong variations with time. Such variations were observed during the first months of operation of *G3* at DESY and then disappeared after approximatively one year of operation to reach a stable state of ~ 0.025 mA. We think [6] that these variations are a signature of the conditioning process (of both the back plate of the RF gun and the surface of the photocathode). The dark current measured at DESY with *G4* is in the same order of magnitude than what was previously measured at FNAL.

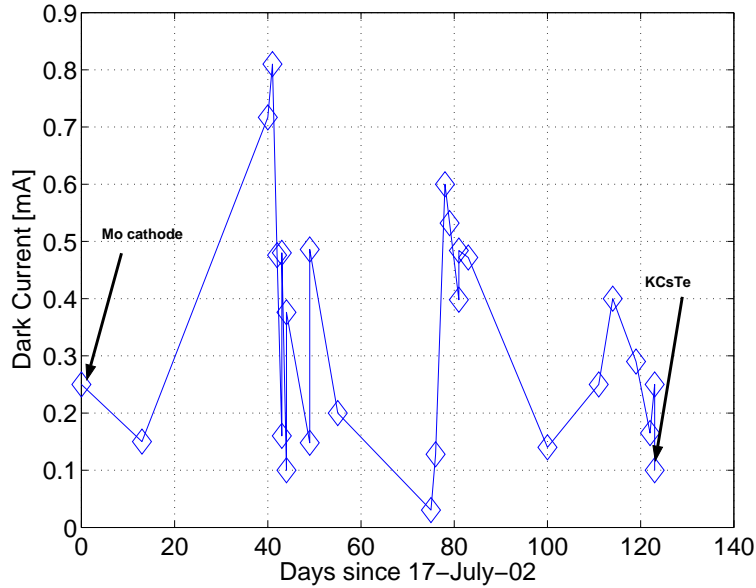


Fig. 4: Dark current evolution in *G4* during the operation at DESY for a peak electric field on the gun of $E_0 = 35$ MV/m and a current of $I_p = 216$ A, $I_s = 110$ A in the solenoids.

3.3 Breakdown observations

During the conditioning of *G4*, we observed that some RF pulses could not reach their full length because of a cut occurring mainly at the beginning of the pulses. In fact, for these pulses, a high reflected power (> 150 kW) was detected by a diode installed in the directional coupler located at the exit of the circulator. When detected, the high reflected power signal was firing the interlock, preventing the signal of the vector modulator to be amplified and thus cutting the incident RF pulse (see Figure 3). The TTF RF system was set in such a way that four gun reflected power events in a row would need the intervention of an operator to reset the interlock. In the following, these cut pulses are named breakdowns.

During the experiments, the main characteristics (forward power, pulse length, repetition rate, etc..) of each incoming RF pulse were written into a file. A program has been developed in order to do an offline analysis of these files and to get statistics on the breakdowns. A typical output given by this program is presented in Figure 5 which shows the amount and the location of the breakdowns (within the RF pulse) for 600 RF pulses. Pulses without breakdowns are not shown. As depicted in Figure 5, a Rayleigh fit of the distribution has been used to determine the mean time at which the breakdowns occur. The mean time of the breakdowns corresponds to the peak of the fit.

To compute the breakdowns, the program uses the ADC signal of the forward power (coming from the directional coupler located upstream of the RF gun) to compute the length of the incident RF pulse. The pulses that do not reach their full length are then counted as breakdowns. It is interesting to note that the breakdowns are not distributed equally along the RF pulse. Most of the breakdowns occur at the beginning of the RF pulse, after 10 to 20 μs .

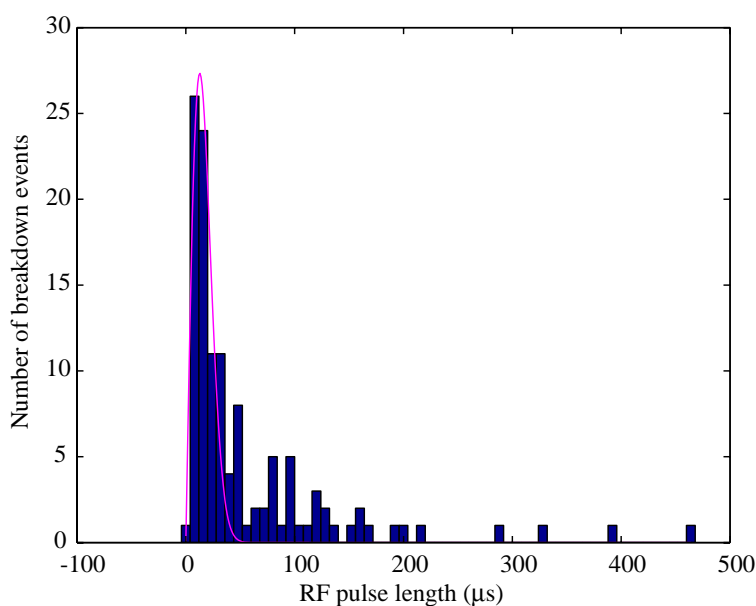


Fig. 5: Distribution of the time when a breakdown occurs. The total number of events is 600 and events without breakdowns are not shown. The distribution is fit to a Rayleigh distribution.

4. Breakdown statistics

During the last week of operation of TTF1(12-17 Nov 2002), we measured the dependency of the breakdowns with respect to the forward power, the RF pulse length and the repetition rate. These measurements were taken using the program described in the previous paragraph and are reported in the following.

4.1 Breakdowns versus Forward Power

Figure 6 shows the percentage and mean time of breakdowns measured as a function of the forward power for an RF pulse length of $500 \mu\text{s}$, a repetition rate of 1 Hz and operating with (a) sharp and (b) smooth RF pulses rising edges. The power reported has been measured with a calibrated powermeter at the directional coupler located upstream of the RF gun. For the measurements presented in Figure 6(a) the feedback loop was open leading to a "rectangular" RF pulse while for Figure 6(b) the feedback loop was closed implying an RF pulse with a slow rising edge. Each point of measurement is a statistic on 600 RF pulses. Both measurements were done the same day, taking 5 hours for the case "open loop" and 3 hours for the case "closed loop".

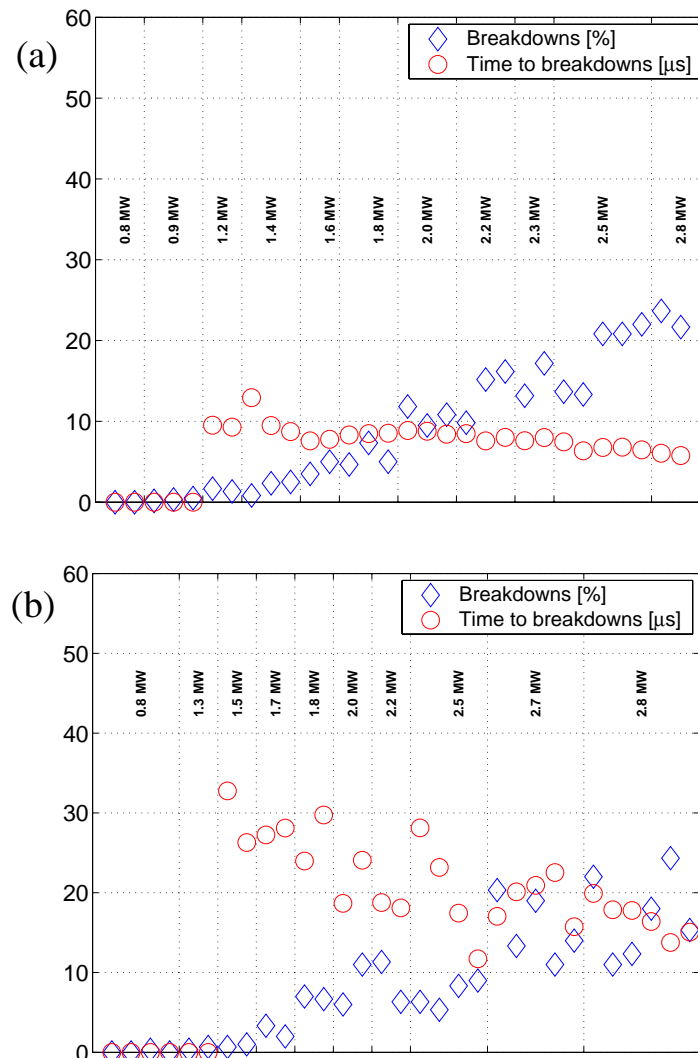


Fig. 6: Breakdowns statistics versus forward power for an RF pulse length of $500 \mu\text{s}$, a repetition rate of 1 Hz and a (a) sharp and (b) smooth RF pulse rising edge.

Figure 6(a) shows that breakdowns appear at a maximum forward power of 1.2 MW for a rectangular RF pulse. The mean time of the breakdowns is then around $\sim 10 \mu\text{s}$. In case of an RF pulse with a slow rising edge the breakdowns appear at a higher maximum forward power ($\sim 1.5 \text{ MW}$) and longer mean time $\sim 30 \mu\text{s}$. For both cases, the percentage of breakdowns increase with respect to the forward power, up to $\sim 25\%$ at 2.8 MW. It is interesting to notice that the mean time of the breakdowns decrease by a factor of 2 with respect to the forward power, from $\sim 10 \mu\text{s}$ to $\sim 5 \mu\text{s}$ (loop open) and from $\sim 30 \mu\text{s}$ to $\sim 15 \mu\text{s}$ (closed open).

Figures 7 represents the gradient in the RF gun for a forward power of 1.5 MW (Figure 7(a)) and 2.2 MW (Figure 7(b)) while operating "open loop" (red curves) and "close loop" (black curves). From these figures, we can see that below $30 \mu\text{s}$, the gradient in the RF gun is almost identical for the cases "open loop" and "closed loop". For this reason, we do not suspect the gradient to be responsible for the shorter mean time of the breakdowns measured while operating "open loop" compared to the case "closed loop". Figure 7(a) indicates also that, while operating "closed loop" at 1.5 MW of forward power, the gradient presented a bump in the first $50 \mu\text{s}$. This bump was not present in the operation "closed loop" at 2.7 MW. We suspect the parameters of feedback loop to not have been properly adjusted for the case 1.5 MW. From these observations, it seems that operating the RF gun with a sharp (feedback loop open) or slow (feedback loop closed) RF pulse rising edge do not impact the breakdowns statistics significantly.

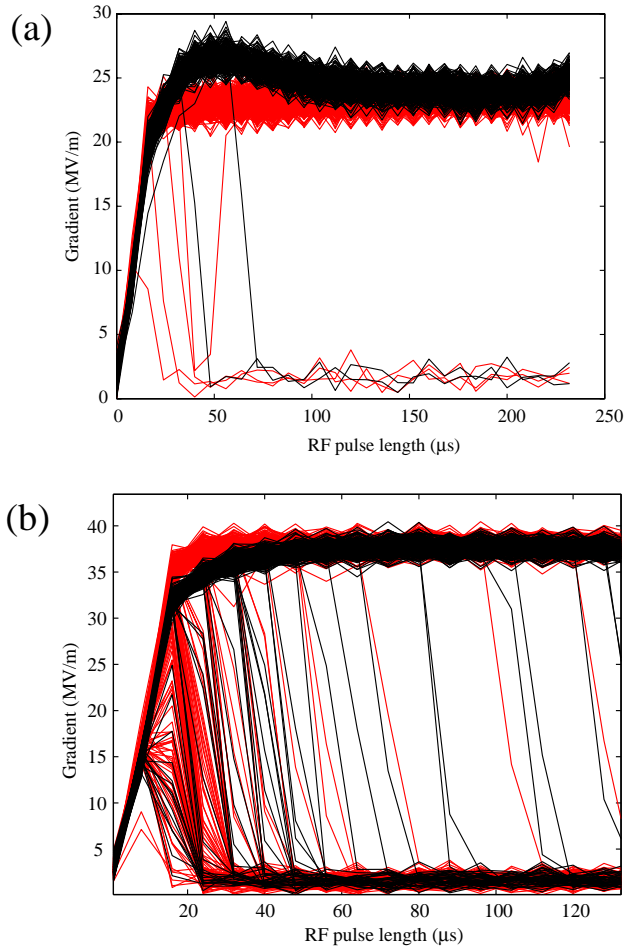


Fig. 7: RF gun gradient in the cases closed loop (red) and open loop (black) for a forward power of (a) 1.5 MW and (b) 2.7 MW.

The same measurement than the one presented in Figure 6(b) has been repeated and is reported in Figure 8. In this experiment we increased the forward power to a maximum of 2.8 MW and then we decreased it. We can notice from Figure 8(a) that the breakdown rates were measured significantly lower while lowering the incident power and at the same time the mean time of the breakdowns was increasing.

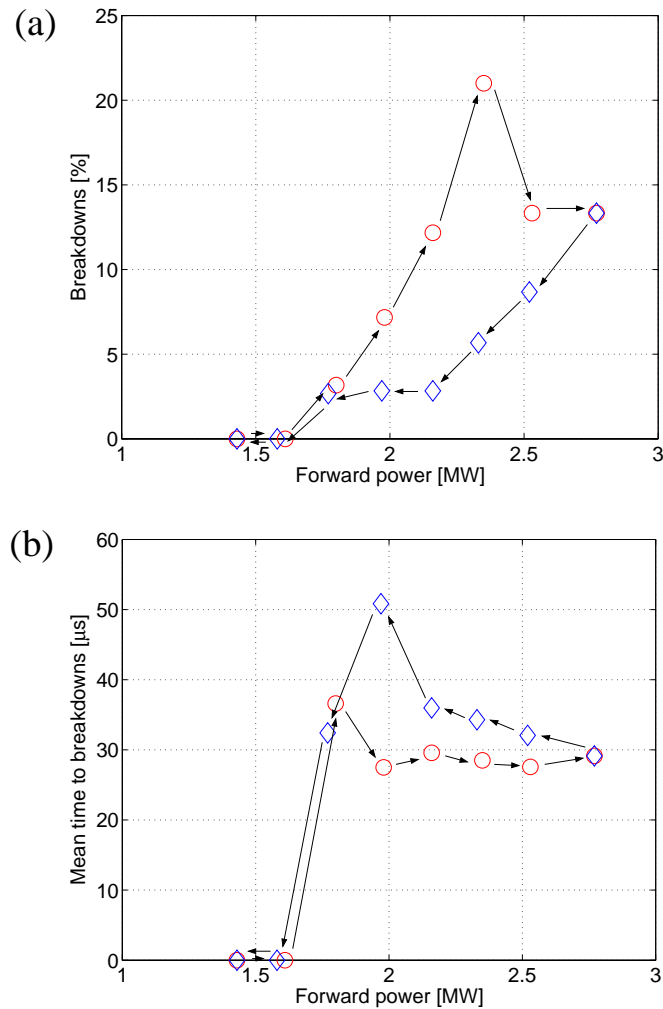


Fig. 8: Breakdowns statistics versus forward power for an RF pulse length of 500 μs and a repetition rate of 1 Hz. The arrows indicate the direction of measurements.

4.2 Breakdowns versus RF pulse length

Figures 9 show breakdown statistics as a function of RF pulse length for a constant forward power of 2.2 MW at the RF gun and for a repetition rate of (a) 0.1 Hz, (b) 1 Hz and (c) 2 Hz. Each point represents a statistics on 5 measurements, each measurement being a statistics on 600 RF pulses. For each measurement point the water temperature has been adjusted to minimize the reflected power to 90 kW. The feedback loop was open in case of 0.1 Hz and closed in case of 1 Hz and 2 Hz.

It is interesting to notice in Figure 9(a) and 9(b) that the percentage of breakdowns seems to be inversely proportional to the repetition rate. In fact, the maximum percentage of breakdowns measured was $\sim 40\%$ at 0.1 Hz, 20% at 1 Hz and 5% at 2 Hz. The mean time of the breakdowns seems to increase with respect to the RF pulse length from $\sim 5\mu\text{s}$ to $\sim 15\mu\text{s}$ in the case 0.1 Hz and from $\sim 10\mu\text{s}$ to $\sim 30\mu\text{s}$ in the cases 1 Hz and 2 Hz. It has been difficult to understand this decrease of the breakdowns rates. We

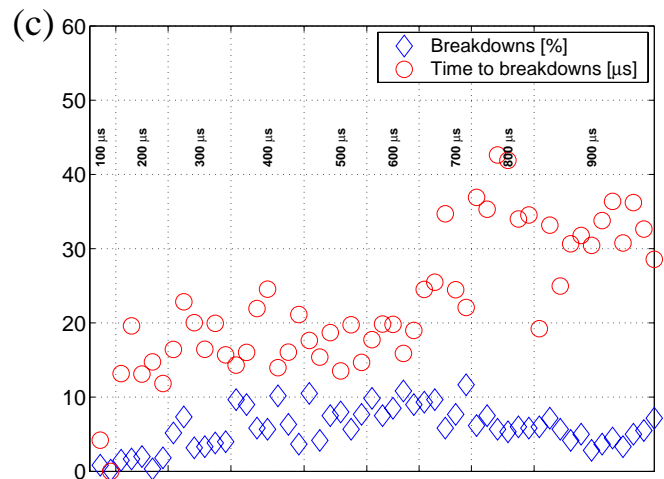
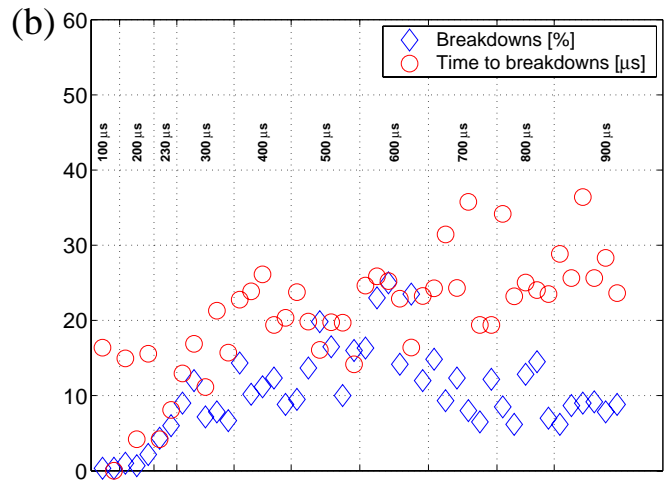
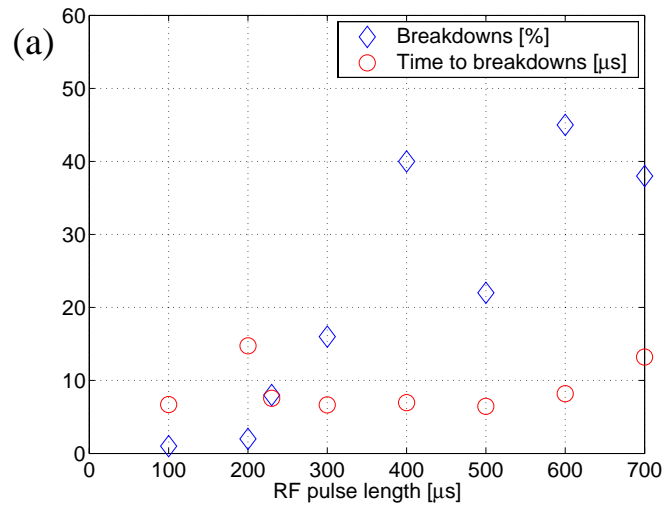


Fig. 9: Breakdowns statistics versus the RF pulse length for a forward power of 2.2 MW and at (a) 0.1 Hz (b) 1 Hz and (c) 2 Hz repetition rate

could think from these results that the following pulse remembers the previous one. As discussed in the following section, simulations showed that this does not seem to be the case for the heating due to the RF pulse.

5. Breakdowns: Where and Why ?

Where ?

Breakdowns were also observed during the operation of *G3* at TTF. These breakdowns were leading to pulse shortening and sparks reducing effectively the effective beam time of TTF for pulse length longer than $300\mu\text{s}$. Piezo-electric ultrasonic sensors were then used to locate the breakdowns in this RF gun [1]. In fact, the breakdowns generate an acoustic signal which amplitude and arrival time is measured with several sensors spread out over the outer surface of the gun and waveguides. In the case of *G3* the breakdowns have been located in the RF coupling slot, between the waveguide and the full cell. The same experiment has been done to locate the breakdowns in *G4* and, as for *G3*, the breakdowns were located in the coupling slot.

Why ?

In the following, we try to explain the origin of the breakdowns. As mentioned in section 2., during the tuning of the RF gun the coupling slot edges were kept sharp. We estimate the roundness of these edges to be in the order of 0.1 mm. HFSS [7] simulations showed that in the presence of RF power in the cavity, the edges of the coupling slot facing the interior of the RF gun are exposed to a strong surface magnetic field in the order of 375 kA/m (for 2.2 MW of RF power and an RF pulse length of $900\mu\text{s}$). This magnetic field induces eddy current which induces heat and this heat is dissipated into the metal and induces stresses. Figure 10(a) shows the temperature distribution in the coupling slot (for an RF pulse of 2.2 MW and $900\mu\text{s}$) and Figure 10(b) the corresponding stress distribution. The peak temperature is then 420°C and the stress is 170 MPa. We think that the abrupt increase of the surface temperature is the most probable reason for the breakdowns. In fact, we suspect field emission created at surface cracks opened due to resistive stress. The starting point for copper of plastic deformation is between 70 to 250 MPa, so the probability of plastic deformation due to RF pulse heating is high enough. Multipactoring and/or sparks can then develop, which then led to a reflection of the incident power.

Figure 11 shows the temperature evolution of the edges of the coupling slot for an RF pulse length of $900\mu\text{s}$ and a forward power of 2.2 MW : in the first 0.1 s, the temperature decreases from 420°C to $\sim 30^\circ\text{C}$. We can then conclude from this study that there is no influence of previous pulses on the following ones. Figure 12 is a reconstructed picture of the coupling slot of the RF gun *G3*. These pictures were taken after dismounting the RF gun from TTF at FNAL and show that cracks are located around the coupling slot, mostly in the bottom left and right of the picture. As discussed, we suspect the RF pulse heating to be responsible for these cracks. It is important to notice that the opening of the coupling slot of the RF gun *G3* has been done by hand (using mainly a file) making imperfections in the surface of the slot which could led to stronger stresses in the presence of RF pulses than predicted by ANSYS. We expect cracks to be present as well in the coupling slot of the RF gun *G4* but due to the fact that the machining of the coupling slot of the RF gun *G4* has been done using a machine tool (as explained in Section 2.) we expect the surface of the coupling slot of *G4* to be much smoother than *G3* and therefore the cracks to be less important in intensity and density with *G4* than with *G3*.

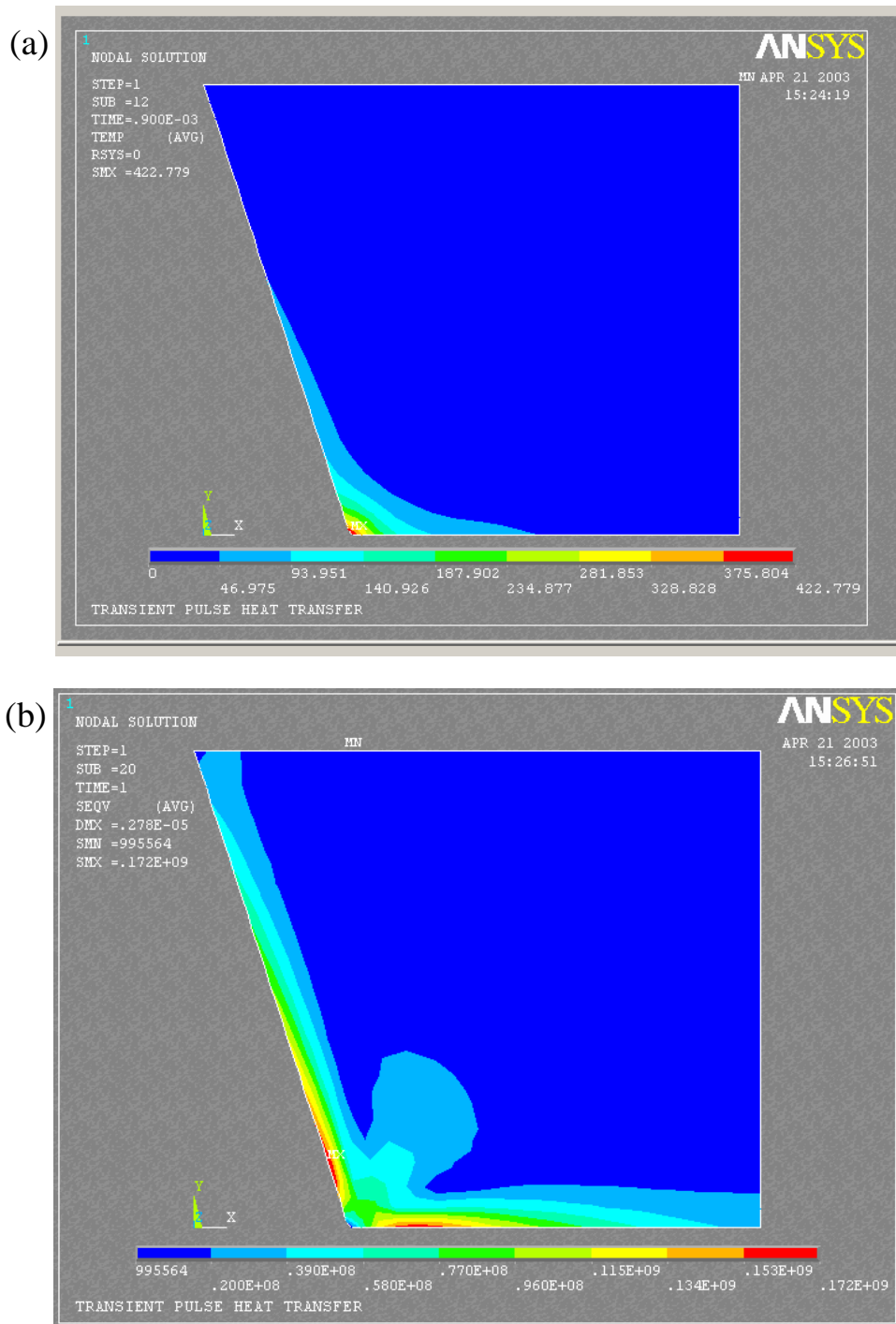


Fig. 10: ANSYS [8] simulation of a (a) temperature ($^{\circ}\text{C}$) and (b) stress (Pa) distribution around the coupling slot edge. Forward RF power = 2.2 MW, RF pulse length = 900 μs .

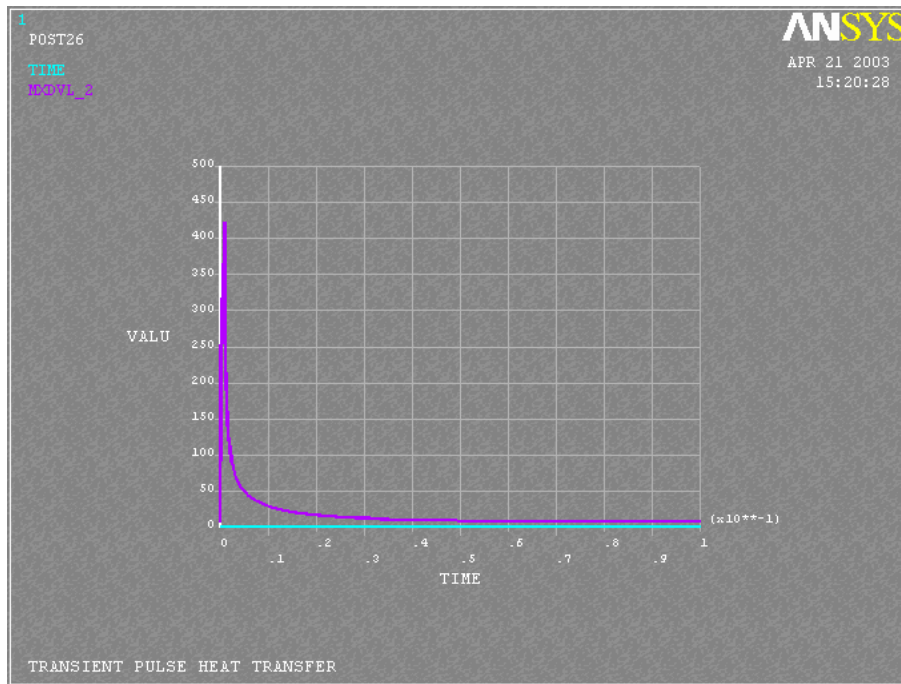


Fig. 11: ANSYS [8] simulation of the temperature evolution in the coupling slot edges after an RF pulse of $900 \mu\text{s}$ and 2.2 MW. The abscise scale is 0.1 s per graduation.



Fig. 12: Reconstructed picture of the coupling slot of the RF gun *G3* (view from the inside). Courtesy of M. Huening, FNAL.

6. Conclusion

RF breakdowns have been observed in the Fermilab RF gun for RF powers of more than 1.2 MW and RF pulse length of more than 100 μ s. These breakdowns have been located in the coupling slot between the waveguide and the full cell and we think they are caused by RF pulse heating inducing an abrupt temperature rise and the development of local stress. The breakdowns probability increases sharply with the RF power and the RF pulse length and does not depend significantly on the sharpness of the rising RF pulse edge. The breakdowns rate is inversely proportional to the repetition rate, going from $\sim 40\%$ at 0.1 Hz, to 20% at 1 Hz and 5% at 2 Hz for a forward power of 2.8 MW. The mean time of the breakdowns occurs at $\sim 10\mu$ s for an RF pulse with sharp rising edge and at $\sim 20 - 30\mu$ s for an RF pulse with smooth rising edge.

A new design of the coupling slot with more round edges and/or using tungsten [9] is a possible cure to the breakdowns. In fact, the melting point of tungsten is three times higher than copper. Finally, we would like to mention that similar effects have been observed in copper structures at SLAC [10] and that after the end of the TTF phase 1 runs, both RF guns have been sent back to Fermilab where these studies are continued.

7. Acknowledgement

We thank M. Ross and J. Nelson from SLAC for tracking down the breakdown location with their microphone system, H. Schlarb for his help with the data acquisition and K. Floettmann for useful discussions and comments.

References

- [1] J. Nelson and M. Ross, "Studies of TTF RF Photocathode Gun using acoustic sensors ", TESLA note 2001-35, November 2001.
- [2] J.-P. Carneiro *et al.* "Experimental studies of RF breakdowns in the coupler of the TTF RF gun", Proceedings of the Particle Accelerator Conference 2003, Portland, Oregon.
- [3] L. Serafini, "Improving the beam quality of RF guns by correction of RF and space-charge effects", AIP Proceedings 279, p. 645-674, 1993.
- [4] D. Edwards, "TESLA Test Facility Linac", Design Report, TESLA-95-01, 1995.
- [5] POISSON/SUPERFISH group of codes, Los Alamos, Version 4.2, 1993.
- [6] S. Schreiber *et al* "On the photocathodes used at the TTF photoinjector", Proceedings of the Particle Accelerator Conference 2003, Portland, Oregon.
- [7] See <http://www.ansoft.com/products/hf/hfss/>
- [8] See <http://www.ansys.com>
- [9] H. H. Braun, CLIC Note 535, Sept. 2002.
- [10] D. P. Pritzkau, RF Pulsed Heating, SLAC-Report-577, Dec. 2001.